THE JOURNAL OF BIOLOGICAL CHEMISTRY
Vol. 280, No. 31, Issue of August 5, pp. 28337–28346, 2005
Printed in U.S.A.

Cyclooxygenase-2-mediated DNA Damage*[S]

Received for publication, April 18, 2005, and in revised form, June 14, 2005
Published, JBC Papers in Press, June 17, 2005, DOI 10.1074/jbc.M504178200

Seon Hwa Lee‡, Michelle V. Williams‡, Raymond N. DuBois§, and Ian A. Blair‡¶

From the ‡Center for Cancer Pharmacology, University of Pennsylvania, Philadelphia, Pennsylvania 19104-6160 and §Department of Medicine, Vanderbilt-Ingram Cancer Center, Vanderbilt University Medical Center, Nashville, Tennessee 37232-6838

Rat intestinal epithelial cells that express the cyclooxygenase-2 (COX-2) gene permanently (RIES cells) were used as a model of *in vivo* oxidative stress. A targeted lipidomics approach showed that 15(*S*)-hydroxyeicosatetraenoic acid (15(*S*)-HETE) was the major hydroxylated non-esterified lipid formed in unstimulated intact cells. The corresponding hydroperoxide, 15(*S*)-hydroperoxyeicosatetraenoic acid (15(*S*)-HPETE) undergoes homolytic decomposition to the DNA-reactive bifunctional electrophile 4-oxo-2(*E*)-nonenal, a precursor of heptanone-etheno-2′-deoxyguanosine. This etheno adduct was identified in the DNA of RIES cells. A dose-dependent increase in adduct levels was observed in the presence of vitamin C. This suggested that vitamin C increased lipid hydroperoxide-mediated 4-oxo-2(*E*)-nonenal formation in the cells. The selective COX-2 inhibitor NS-398 was protective against cellular DNA damage but was less effective if vitamin C was present. Prostaglandin E_2 and 15(*S*)-HETE biosynthesis were completely inhibited by 110 μM NS-398 in the intact RIES cells. No inhibition of COX-1 was detected in the wild-type RIE cells at this concentration of NS-398. Arachidonic acid treatment of RIES cell lysates and ionophore stimulation of intact RIES cells produced significantly more 15(*R*)-HETE than the untreated intact cells. These preparations also both produced 11(*R*)-HETE, which was not detected in the intact cells. Aspirin treatment of the intact unstimulated RIES cells resulted in the exclusive formation of 15(*R*)-HETE in amounts that were slightly higher than the original 15(*S*)-HETE observed in the absence of aspirin, implying that significant amounts of 15(*R*)-HPETE had also been formed. 15(*R*)-HPETE should give exactly the same amount of heptanone-etheno-2′-deoxyguanosine as its 15(*S*)-enantiomer. However, no increase in heptanone-etheno adduct formation occurred in the aspirin-treated cells. The present study suggests a potential mechanism of tumorigenesis that involves DNA adduct formation from COX-2-mediated lipid peroxidation rather than prostaglandin formation. Therefore, inhibition of COX-2-mediated lipid hydroperoxide formation offers a potential therapeutic alternative to COX-2 inhibitors in chemoprevention strategies.

Lipid hydroperoxides are formed enzymatically through the action of COXs[1] and LOXs on ω-3 and ω-6 polyunsaturated fatty acids (1–3). They are produced non-enzymatically by the action of reactive oxygen species when cellular reducing equivalents are compromised such as during oxidative stress (4). With AA as the substrate, COX-1 and COX-2 both produce 15-HPETE (Scheme I). The 15-HPETE is subsequently reduced to 15-HETE through the peroxidase activity of the COXs (1, 2) or by GSH-dependent peroxidases that are present in the cellular milieu (5) (Scheme I). COX-1 and COX-2 convert AA to 15-HETE as a mixture of (*R*)-and (*S*)-enantiomers (6–8). AA is also an excellent substrate for 15-LOX-1 (9) and 15-LOX-2 (10), which both produce exclusively 15(*S*)-HPETE that is reduced to 15(*S*)-HETE, whereas reactive oxygen species-mediated peroxidation of AA results in the formation of a complex mixture of HPETEs that are reduced to racemic HETEs including 15(*R*)- and 15(*S*)-HETE (4).

The major initial LA-derived products of COX-2-mediated metabolism are 9(*R*)-HPODE and 13(*S*)-HPODE (Scheme I). HPODEs are subsequently reduced to the corresponding 9(*R*)- and 13(*S*)-HODEs in a similar manner to HPETEs (1, 2) (Scheme I). LA is a substrate for both 15-LOX-1 (9) and 15-LOX-2 (10) where it exclusively produces 13(*S*)-HPODE that is subsequently reduced to 13(*S*)-HODE. Reactive oxygen species-mediated peroxidation of LA results in a complex mixture of HPODEs that are reduced to racemic HODEs including 13(*R*)- and 13(*S*)-HODE (4). In a previous study we examined vitamin C-mediated homolytic decomposition of 13(*S*)-HPODE and characterized the major DNA reactive α,β-unsaturated aldehydic bifunctional electrophiles as HPNE, ONE, HNE, *t*-EDE, and *c*-EDE (11). These bifunctional electrophiles were derived from the ω terminus of the 13(*S*)-HPODE. The same bifunctional electrophiles were shown to arise from 15(*S*)-HPETE (12), whereas only HPNE, ONE, and HNE were formed from 5(*S*)-HPETE (13). We have recently confirmed that DODE is a

* This work was supported by National Institutes of Health Grants CA95586 (to I. A. B.) and DK047297 (to R. N. D.). The costs of publication of this article were defrayed in part by the payment of page charges. This article must therefore be hereby marked "*advertisement*" in accordance with 18 U.S.C. Section 1734 solely to indicate this fact.

[S] The on-line version of this article (available at http://www.jbc.org) contains supplemental material.

¶ To whom correspondence should be addressed: Center for Cancer Pharmacology, 854 BRB II/III, 421 Curie Blvd., University of Pennsylvania, Philadelphia, PA 19104-6160. Tel.: 215-573-9880; Fax: 215-573-9889; E-mail: ian@spirit.gcrc.upenn.edu.

[1] The abbreviations used are: COX, cyclooxygenase; AA, arachidonic acid; *c*-EDE, *cis*-4,5-epoxy-2(*E*)-decenal; *t*-EDE, *trans*-4,5-epoxy-2(*E*)-decenal; DODE, 9,12-dioxo-10-dodecenoic acid; dGuo, 2′-deoxyguanosine; MS, mass spectrometry; 5-HETE, 5-hydroxy-6,8,11,14-(*E,Z,Z,Z*)-eicosatetraenoic acid; 8-HETE, 8-hydroxy-5,9,11,14-(*Z,E,Z,Z*)-eicosatetraenoic acid; 11-HETE, 11-hydroxy-5,8,12,14-(*Z,Z,E,Z*)-eicosatetraenoic acid; 12-HETE, 12-hydroxy-5,8,10,14-(*Z,Z,E,Z*)-eicosatetraenoic acid 15-HETE, 15-hydroxy-5,8,11,14-(*Z,Z,Z,E*)-eicosatetraenoic acid; HNE, 4-hydroxy-2(*E*)-nonenal; HPETE, hydroperoxyeicosatetraenoic acid; HPNE, 4-hydroperoxy-2(*E*)-nonenal; HPODE, hydroperoxyoctadecadienoic acid; 8-*iso*-$PGF_{2\alpha}$, 9α,11α,15(*S*)-trihydroxy-(8β)-prosta-5*Z*,13*E*-dien-1-oic acid; LC, liquid chromatography; LOX, lipoxygenase; MOPS, 3-morpholinopropanesulfonic acid; MRM, multiple reaction monitoring; NS-398, *N*-[2-cyclohexyloyl-4-nitrophenyl] methane sulfonamide; ONE, 4-oxo-2(*E*)-nonenal; PFB, pentafluorobenzyl; PG, prostaglandin; RIE rat intestinal epithelial; RIES, RIE cells that express the COX-2 gene permanently; RPMI, Roswell Park Memorial Institute; WT, wild type; LA, linoleic acid; FBS, fetal bovine serum; HPLC, high performance liquid chromatography; RT, reverse transcription; APCI, atmospheric pressure chemical ionization; LA, linoleic acid.

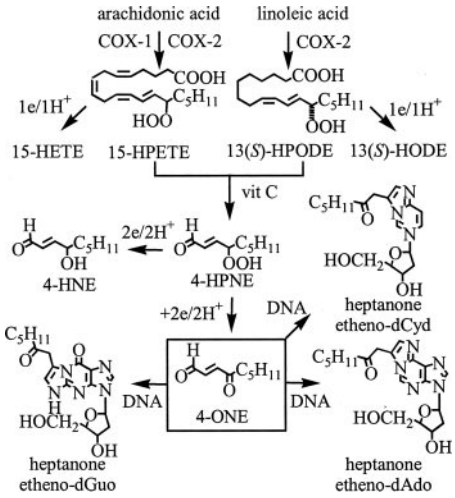

SCHEME 1. **Scheme for the formation of bifunctional electrophiles from lipid hydroperoxides.** *dAdo*, 2′-deoxyadenosine; *dCyd*, 2′-deoxycytidine; *dGuo*, 2′-deoxyguanosine.

major product derived from the α terminus of 13(*S*)-HPODE (14). The formation of this bifunctional electrophile was suggested from isolation of 9-carboxynonan-2-one-etheno DNA adducts from the decomposition of 13(*S*)-HPODE in the presence of DNA (15). DODE can only arise from LA-derived lipid hydroperoxides (14).

Lipid hydroperoxide-derived bifunctional electrophiles are formed by three distinct pathways (Scheme I). The first pathway involves α-cleavage of an alkoxy radical and results in formation of *t*-EDE and *c*-EDE (16, 17). The second pathway involves formation of HPNE, which undergoes reduction to HNE or a 2-electron oxidation to ONE (11–13, 18–20). The third pathway appears to involve the intermediate formation of 9-hydroperoxy-12-oxo-10-decenoic acid, which undergoes a 2-electron oxidation to DODE (14), a reaction observed in the conversion of HPNE to ONE (11–13).

In a series of studies, ONE was shown to mediate the formation of heptanone-etheno-dGuo, heptanone-etheno-dAdo, and heptanone-etheno-dCyd adducts (21–24), whereas EDE was found to mediate the formation of unsubstituted etheno-dGuo and etheno-dAdo adducts (17). However, HPNE is almost 10 times more efficient than EDE in forming unsubstituted etheno adducts (25). Therefore, HPNE appears to the major source of unsubstituted etheno adducts that arise from lipid peroxidation. Etheno-dGuo is mutagenic in mammalian cells (AA8 Chinese hamster ovary), inducing base pair mutations, with a preference for G to A transitions (26). Etheno-dAdo is more mutagenic in human cells (HeLa) than 8-oxo-dGuo, inducing A to T transversions in experiments using modified double- and single-stranded DNA substrates (27). In contrast to ONE, HNE is not very reactive toward DNA (28). However, both HNE and ONE can readily modify nucleophilic amino acid residues in proteins (29–33). For example ONE forms a novel cyclic peptide in histone H4 by reaction with proximal histidine and lysine residues in the protein (31). DODE is the presumed intermediate in the formation of 9-carboxynonan-2-one-etheno DNA adducts with dGuo (14), 2′-deoxyadenosine, and 2′-deoxycytidine (15).

Numerous studies have implicated COXs as mediators of carcinogenesis. In addition, there is a correlation between the use of non-steroidal anti-inflammatory drugs and a reduction in risk for colon and breast cancer (34–36). COX-2 is up-regulated in many tumors when it is absent from unaffected surrounding tissue (37). COX-mediated formation of PGs has long been assumed to play a role in tumorigenesis (38). However, little attention has been given to the potential for the formation of genotoxic bifunctional electrophiles that result from COX-mediated lipid hydroperoxide formation. We reasoned that cells permanently expressing the COX-2 gene (RIES cells) would produce HPETEs or HPODEs by COX-2-mediated metabolism of AA or LA. This would then make it possible to test whether the intracellular formation of lipid hydroperoxides could induce DNA adduct formation. RIE cells were chosen because they have been used extensively in studies of the mechanism by which COX-2 is involved in adhesion, cell proliferation, and apoptosis (39, 40). Using RIES cells, it was possible to determine whether the lipid hydroperoxides were derived from AA or from LA by analyzing the resulting HETEs and HODEs using a targeted lipidomics approach that we developed recently (41). This method is based on stable isotope dilution LC/electron capture APCI/MS/MS methodology, which makes it possible to employ normal phase chiral chromatography with extremely high sensitivity (42). Specificity of the approach comes from the use of MRM analysis of a specific parent ion and a specific product ion for each analyte coupled with enantio-selective separation of the resulting lipids. If the lipid hydroperoxides were derived from AA it would then be possible (using specific inhibitors) to determine whether they arose from constitutive COX-1 or from COX-2. We report the use of targeted chiral lipidomics methodology to examine lipid hydroperoxide formation in RIES cells together with stable isotope dilution LC/MS quantitation of DNA adducts that were formed. We also report the regulation of DNA adduct formation by vitamin C, which has been shown previously to activate lipid hydroperoxides to endogenous genotoxins *in vitro* (11).

EXPERIMENTAL PROCEDURES

Materials and Reagents—9(*R*)-HODE, 9(*S*)-HODE, 13(*R*)-HODE, 13(*S*)-HODE, 5(*R*)-HETE, 5(*S*)-HETE, 8(*R*)-HETE, 8(*S*)-HETE, 11(*R*)-HETE, 11(*S*)-HETE, 12(*R*)-HETE, 12(*S*)-HETE, 15(*R*)-HETE, 15(*S*)-HETE, 11β-PGE_2, 8-*iso*-PGE_2, PGE_2, PGD_2, $PGF_{2\alpha}$, 11β-PGF_2, 8-*iso*-$PGF_{2\alpha}$, [$^2H_4$]PGE_2, [$^2H_4$]$PGF_{2\alpha}$, 9(*S*)-[$^2H_4$]HODE, 13(*S*)-[$^2H_4$]HODE, 5(*S*)-[$^2H_8$]HETE, 12(*S*)-[$^2H_8$]HETE, and 15(*S*)-[$^2H_8$]HETE were purchased from Cayman Chemical Co. (Ann Arbor, MI). Ammonium acetate, vitamin C, diisopropyl ethylamine, DNase I, zinc chloride, and PFB-Br were purchased from Sigma-Aldrich. RPMI and FBS were supplied by Invitrogen. HPLC grade water, acetonitrile, hexane, methanol, and isopropanol were obtained from Fisher. Gases were supplied by BOC Gases (Lebanon, NJ).

MS—A Finnigan TSQ 7000 triple stage quadrupole mass spectrometer (Thermo Electron, San Jose, CA) equipped with an APCI source was used in the studies. For full-scan and MRM analyses, unit resolution was maintained for both parent and product ions. For the lipidomics profile, the instrument was operated in the negative ion mode. Operating conditions for the TSQ 7000 were vaporizer temperature at 500 °C and heated capillary temperature at 230 °C, with the corona discharge needle set at 16 μA. The sheath gas (nitrogen) and auxiliary gas (nitrogen) pressures were 40 p.s.i. and 10 (arbitrary units), respectively. Collision-induced dissociation was performed using argon as the collision gas at 2.7 mtorr in the Rf-only quadrupole. Targeted chiral LC/electron capture APCI/MRM/MS analysis was conducted using PFB derivatives of 21 lipids and 7 heavy isotope analog internal standards. The following MRM transitions were used: 9(*R*)- and 9(*S*)-HODE-PFB, *m/z* 295 → 171 (collision energy, 20 eV); 9(*S*)-[$^2H_4$]HODE-PFB, *m/z* 299 → 172 (collision energy, 18 eV); 13(*R*)- and 13(*S*)-HODE-PFB, *m/z* 295 → 195 (collision energy, 20 eV); 13(*S*)-[$^2H_4$]HODE-PFB, *m/z* 299 → 198 (collision energy, 20 eV); 5(*R*)- and 5(*S*)-HETE-PFB, *m/z* 319 → 115 (collision energy, 15 eV); 5(*S*)-[$^2H_8$]HETE-PFB, *m/z* 327 → 116 (collision energy, 16 eV); 8(*R*)- and 8(*S*)-HETE-PFB, *m/z* 319 → 155 (collision energy, 16 eV); 11(*R*)- and 11(*S*)-HETE-PFB, *m/z* 319 → 167 (collision energy, 16 eV); 12(*R*)- and 12(*S*)-HETE-PFB, *m/z* 319 → 179 (collision energy, 14 eV); 12(*S*)-[$^2H_8$]HETE-PFB, *m/z* 327 → 184 (collision energy, 14 eV); 15(*R*)- and 15(*S*)-HETE-PFB, *m/z* 319 → 219 (collision energy, 15 eV); 15(*S*)-[$^2H_8$]HETE-PFB, *m/z* 327 → 226 (collision energy, 15 eV); PGE_2-PFB, PGD_2-PFB, 11β-PGE_2-PFB, 8-*iso*-PGE_2-PFB, *m/z* 351 → 271 (collision energy, 20 eV); [$^2H_4$]PGE_2-PFB, *m/z* 355 → 275 (collision energy, 20 eV); 11β-PGF_2-PFB, $PGF_{2\alpha}$-PFB,

8-iso-$PGF_{2\alpha}$-PFB, *m/z* 353 → 309 (collision energy, 22 eV); [$^2H_4$]$PGF_{2\alpha}$-PFB, *m/z* 357 → 313 (collision energy, 20 eV).

For DNA adduct analysis, the instrument was operated in the positive ion mode. The TSQ 7000 operating conditions were vaporizer temperature at 550 °C and heated capillary temperature at 160 °C, with the corona discharge needle set at 8 μA. The sheath gas (nitrogen) and auxiliary gas (nitrogen) pressures were 80 p.s.i. and 3 (arbitrary units), respectively. Collision-induced dissociation was performed using argon as the collision gas at 2.7 mtorr in the Rf-only quadrupole. LC/MRM/MS analysis was conducted using PFB derivatives. The following MRM transitions were monitored: heptanone-etheno-dGuo-PFB (*m/z* 584 → 468) and [$^{15}N_5$]-labeled heptanone-etheno-dGuo-PFB (*m/z* 589 → 473).

LC—Normal phase chiral LC/APCI/MS analysis was conducted using a Waters Alliance 2690 HPLC system (Waters Corp., Milford, MA). A Chiralpak AD-H column (250 × 4.6-mm inner diameter, 5 μm; Daicel Chemical Industries, Ltd., Tokyo, Japan) was employed for gradient 1 with a flow rate of 1.0 ml/min. Solvent A was hexane, and solvent B was methanol/isopropanol (1:1, v/v). Gradient 1 was as follows: 2% B at 0 min, 2% B at 3 min, 4% B at 13 min, 30% B at 15 min, 30% B at 20 min, 50% B at 22 min, 50% B at 25 min, and 2% B at 27 min. Separations were performed at 30 °C using a linear gradient.

LC/UV chromatography for DNA bases was conducted using gradient-2 on a Hitachi L-6200A Intelligent Pump equipped with a Hitachi L4000 UV detector (Hitachi, San Jose, CA). The separation employed a Phenomenex Synergi 4-μm polar reverse phase column (250 × 4.6-mm inner diameter, 4 μm). Solvent A was 5 mM ammonium acetate in water, and solvent B was 5 mM ammonium acetate in acetonitrile. Gradient 2 was as follows: 6% B at 0 min, 6% B at 3 min, 20% B at 9 min, 20% B at 10 min, 80% B at 12 min, 80% B at 15 min, 6% B at 17 min, and 6% B at 25 min. The flow rate was 1 ml/min. The separation was performed at ambient temperature using a linear gradient.

LC/APCI/MS analysis of DNA adducts using gradient 3 was performed on a Waters Alliance 2690 HPLC system (Waters Corp.). The separation employed an XTerra C18 column (250 × 4.6-mm inner diameter, 5 μm). Solvent A was 5 mM ammonium acetate in water, and solvent B was 5 mM ammonium acetate in acetonitrile. Gradient-3 was as follows: 6% B at 0 min, 6% B at 3 min, 20% B at 9 min, 20% B at 13 min, 40% B at 22 min, 70% B at 27 min, 80% B at 28 min, 80% B at 32 min, and 6% B at 34 min. The flow rate was 1.0 ml/min. The separation was performed at ambient temperature using a linear gradient.

Incubations of Intact RIES Cells with NS-398 and Aspirin—Rat intestinal epithelial cells transfected with COX-2 (RIES cells) were obtained from Dr. R. N. DuBois (Vanderbilt University). Cells were cultured in RPMI supplemented with 10% FBS, 2 mM glutamine, 100,000 units/liter penicillin, and 100,000 units/liter streptomycin until almost confluent. The medium was removed and replaced with medium containing NS-398 (55 or 110 μM), NS-398 (55 or 110 μM) and vitamin C (0.1 mM), aspirin (200 μM), or aspirin (200 μM) and vitamin C (0.1 mM). Cells were then incubated for 24-h at 37 °C.

Incubations of Intact RIES Cells with Vitamin C—RIES cells were cultured in RPMI supplemented with 10% FBS, 2 mM glutamine, 100,000 units/liter penicillin, and 100,000 units/liter streptomycin until almost confluent. The medium was removed and replaced with medium containing increasing amounts of vitamin C (0.00, 0.03, 0.1, 0.5, 1.0, 5.0 mM in water). Cells were then incubated for 24-h at 37 °C.

Extraction of DNA from Intact RIES Cells—DNA isolation from 8 plates of RIES cells (total 8 × 10^6 cells) was performed using a Wako DNA extraction WB kit (Wako Chemicals, Richmond, VA). Briefly, cells were lysed after a 24-h incubation and then treated with an enzyme reaction solution and protease to liberate the DNA from the nucleus. This was followed by the addition of aqueous sodium iodide extraction followed by several wash steps to purify the DNA. Typically 300–500 μg of DNA was obtained. It was hydrolyzed as described below, and normal bases were quantified by LC/UV using gradient 2.

Hydrolysis of DNA and Isolation of Heptanone-Etheno-dGuo—The DNA extracted from 8 plates of RIES cell was combined and dissolved in 10 mM MOPS containing 100 mM NaCl (pH 7.0, 1 ml). DNase I (556 units) dissolved in 10 mM MOPS containing 120 mM $MgCl_2$ (pH 7.0) was added and incubated at 37 °C for 1.5 h. At the end of the incubation, nuclease P1 (15.5 units) was added along with 25 mM $ZnCl_2$, and the incubation continued for a further 2 h at 37 °C. Alkaline phosphatase (30 units) in 0.4 M MOPS (pH 7.8) was then added, and the incubation conducted for 1 h at 37 °C. The samples were filtered through a 0.2-μm Costar cartridge. At this time an aliquot was removed for LC/UV analysis of the bases using gradient 2. Quantitation of DNA bases was carried out by constructing standard curves of known amount of bases. The remaining sample was applied to a solid phase extraction cartridge (6 ml, Supelclean LC-18, Supelco, Bellefonte, PA) that had been pre-washed with acetonitrile (18 ml) and water (18 ml). The cartridge was then washed with water (4 ml) and a methanol/water mixture (1 ml, 5:95 v/v). Heptanone-etheno-dGuo adducts were eluted with an acetonitrile/water mixture (6 ml, 1:1 v/v). The eluates were evaporated to dryness under nitrogen.

Analysis of Heptanone-Etheno-dGuo-Adduct—The eluates containing heptanone-etheno-dGuo were dissolved in acetonitrile (100 μl) and treated with diisopropyl ethylamine/acetonitrile (100 μl, 10:90 v/v) and PFB-Br/acetonitrile (100 μl, 20:80 v/v). The solution was left at room temperature for 1.5 h. It was then evaporated to dryness under nitrogen and dissolved in methanol/methylene chloride (100 μl, 25:75 v/v) and loaded onto a solid phase extraction cartridge (6 ml, Supelclean Si, Supelco) that had been pre-washed with methylene chloride (12 ml). The column was then washed with methanol/methylene chloride (3 ml, 1:99 v/v) and methanol/methylene chloride (1 ml, 5:95 v/v). Heptanone-etheno-dGuo adduct was eluted with methanol/methylene chloride (6 ml, 25:75 v/v) and evaporated to dryness under nitrogen. Finally, the adduct was re-dissolved in acetonitrile/water (100 μl 80:20 v/v). Aliquots (20 μl) were analyzed by LC/APCI/MS/MS using gradient 3. The $^{15}N_5$-labeled internal standards were added to the samples before hydrolysis. Quantitation was performed from a standard curve constructed by the ratio of known amounts of authentic standards and internal standard. For the MRM analysis, parent MH^+ (protonated molecular ion) of endogenous heptanone-etheno-dGuo (*m/z* 584) and $^{15}N_5$-labeled heptanone-etheno-dGuo (*m/z* 589) were monitored. Product ions corresponded to the loss of the 2′-deoxyribose moiety (BH_2^+) from endogenous heptanone-etheno-dGuo (*m/z* 468) and $^{15}N_5$-labeled heptanone-etheno-dGuo (*m/z* 473). Adduct levels were normalized to the number of unmodified DNA bases.

Incubation of Intact RIES Cells with Calcium Ionophore A23187—RIES cells were cultured in RPMI supplanted with 10% FBS, 2 mM glutamine, 100,000 units/liter penicillin, and 100,000 units/liter streptomycin until almost confluent. The medium was removed and replaced with medium containing 0.1% FBS and calcium ionophore A23187 (1 μM final concentration). Cells were then incubated for 1 h at 37 °C.

Incubations of WT RIE Cells with NS-398—Cells were cultured in RPMI supplanted with 10% FBS, 2 mM glutamine, 100,000 units/liter penicillin, and 100,000 units/liter streptomycin until almost confluent. The medium was removed and replaced with medium containing 0.1% FBS or 0.1% FBS and NS-398 (110 μM). Cells were then incubated for 24 h at 37 °C.

Western Blot Analysis of RIES Cells during 24 h of Incubation—Cells were harvested at different time points and washed twice with ice-cold phosphate-buffered saline. They were suspended in lysis buffer containing 50 mM Tris (pH 8.0), 5 mM EDTA, 150 mM NaCl, 0.5% Nonidet P-40, 0.5 mM phenylmethanesulfonyl fluoride, and 1× protease mixture for mammalian tissue (Sigma-Aldrich). The cells were lysed on ice and centrifuged at 10,000 × *g* for 5 min. The supernatant was collected, and the protein concentration was determined by the Quick Start Bradford protein assay kit (Bio-Rad). Cellular protein (10 μg) was loaded on pre-cast 8% NuPAGE Tris-Gly gels (Invitrogen) and then transferred to 0.45 mM nitrocellulose membranes (Invitrogen). The blots were blocked with 5% nonfat milk in Tris-buffered saline (Tris 100 mM (pH 7.5), NaCl 150 mM) containing 0.1% Tween 20 and then incubated with COX-2 antibody (Santa Cruz Biotechnology; Santa Cruz, CA) followed by reaction with secondary antibody, anti-goat (Santa Cruz Biotechnology). Protein bands were visualized with the ECL reagent (Amersham Biosciences).

RT-PCR Analysis of 15-LOX-2 in RIES Cells—Total RNA was extracted from the RIES cell culture samples (Ambion, Austin, TX) according to the manufacturer's instructions. The cells were harvested when cultures had reached full confluence. Conventional RT-PCR reactions were conducted on 2 μg of total RNA. For 15-LOX-2, the primers used were 5′-CCT-GGT-CCA-ATA-TGT-TAC-CAT-3′ (forward) and 5′-CCC-TGG-CTC-CTT-GCT-TAG-CAG-3′ (reverse), which gives a 234-bp amplified product. Thirty cycles of reaction at 56 °C for 30 s, 72 °C for 30 s, and 95 °C for 30 s were carried out on a thermal cycler (PerkinElmer Life Sciences). Wistar rat skin cDNA was used as a positive control for the RT-PCR reaction. It has been demonstrated previously that the 15-LOX-2 mRNA is expressed in this tissue.[2]

RESULTS

Targeted Lipidomics Analysis of Intact RIES Cell Media—LC/electron capture APCI/MRM/MS analysis of 21 targeted lipids from control RIES supernatants (see the supplemental

[2] A. R. Brash, personal communication.

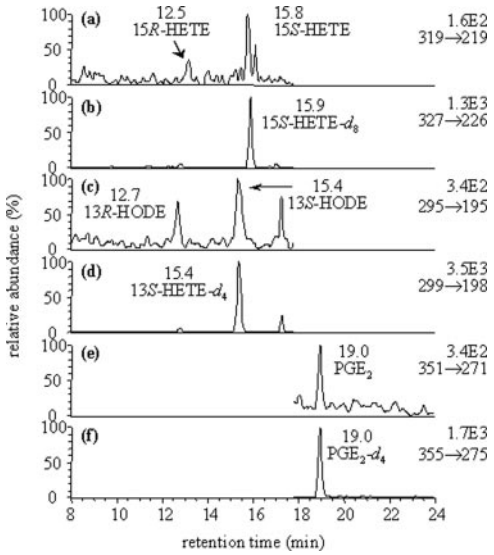

FIG. 1. **Targeted chiral lipidomics analysis of COX-2-derived AA and LA metabolites from RIES cells.** MRM chromatograms are shown for 15(*R,S*)-HETE-PFB (*m/z* 319 → *m/z* 219) (*a*), 15(*S*)-[$^2H_8$]HETE-PFB internal standard (*m/z* 327 → *m/z* 226) (*b*), 13(*R,S*)-HODE-PFB (*m/z* 295 → *m/z* 195) (*c*), 13(*S*)-[$^2H_4$]HODE-PFB internal standard (*m/z* 299 → *m/z* 198) (*d*), PGE_2-PFB (*m/z* 351 → *m/z* 271) (*e*), [$^2H_4$]PGE_2-PFB internal standard (*m/z* 355 → *m/z* 275) (*f*).

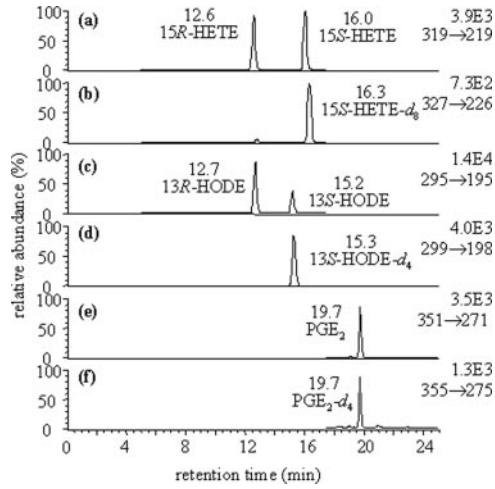

FIG. 2. **Targeted lipidomics using LC/electron capture APCI/MS/MS for analysis of standard lipid PFB derivatives (5 pg each).** MRM chromatograms are shown for 15(*R,S*)-HETE-PFB (*m/z* 319 → *m/z* 219) (*a*), 15(*S*)-[$^2H_8$]HETE-PFB internal standard (*m/z* 327 → *m/z* 226) (*b*), 13(*R,S*)-HODE-PFB (*m/z* 295 → *m/z* 195) (*c*), 13(*S*)-[$^2H_4$]HODE-PFB internal standard (*m/z* 299 → *m/z* 198) (*d*), PGE_2-PFB (*m/z* 351 → *m/z* 271) (*e*), [$^2H_4$]PGE_2-PFB internal standard (*m/z* 355 → *m/z* 275) (*f*).

material) revealed the presence of 15(*S*)-HETE (retention time (rt), 15.8 min), 13(*R*)-HODE (rt, 12.7 min), 13(*S*)-HODE (rt, 15.4 min), and PGE_2 (rt, 19.0 min) (Fig. 1). However, 13(*R*)-HODE and 13(*S*)-HODE were also present at this low level in the media in the absence of the RIES cells. Chromatograms for 15(*R*)-HETE, 15(*S*)-HETE, 13(*R*)-HODE, 13(*S*)-HODE, and PGE_2 derived from LC/electron capture APCI/MRM/MS analysis of a standard mixture of 21 lipids and 7 heavy isotope internal standards is shown in Fig. 2.

Targeted Lipidomics Analysis from Intact RIES Cells—Standard curves were constructed for 15(*S*)- and 15(*R*)-HETE and PGE_2 on three separate days in the range 0.1–5 pmol/10^6 cells, and quality control samples were analyzed (see the supplemental material). Standard curves were constructed for all of the analytes in the range 6.7 pg/ml (0.02 pmol/ml) to 667 pg/ml (2.0 pmol/ml) (1 ml = 10^5 cells). Typical regression lines for 11(*R*)-HETE, 15(*R*)-HETE, 15(*S*)-HETE, and PGE_2 were $y = 301.83x + 132.54$ ($r^2 = 0.9972$), $y = 0.0028x + 0.0285$ ($r^2 = 0.9980$), $y = 0.0049x + 0.0279$ ($r^2 = 0.9999$), and $y = 0.0042x + 0.0067$ ($r^2 = 0.9990$), respectively. The assay was validated by demonstrating for replicate quality control samples a precision of better than ±15% and accuracy between 85 and 115% on three separate days. The limit of detection for 15(*S*)- and 15(*R*)-HODE were 0.15 pmol/10^6 cells and for PGE_2 was 0.10 pmol/10^6 cells (precision was better than ±20%, and accuracy was between 80 and 120% on three separate days). Quantitation of the lipids from three separate incubations of the RIES cells showed the presence of 0.50 ± 0.05 and 0.99 ± 0.07 pmol/10^6 cells of 15(*S*)-HETE and PGE_2, respectively (Table I).

Targeted Lipidomics Analysis of RIES Cells in the Presence of Vitamin C—When the cells were treated with vitamin C (0.1 mM), LC/APCI/MRM/MS analysis of the cell culture medium showed a similar lipidomics profile (Fig. 3) as the RIES supernatants without vitamin C (Fig. 1). Quantitation ($n = 3$) revealed the presence of 15(*S*)-HETE (0.39 ± 0.05 pmol/10^6 cells) and PGE_2 (0.95 ± 0.09 pmol/10^6 cells) (Table I). Therefore, a modest reduction of 15(*S*)-HETE was observed in the vitamin C-treated cells when compared with the untreated cells. There was no effect of vitamin C on PGE_2 biosynthesis.

TABLE I
Amounts of 15(S)-HETE and PGE_2 excreted by RIES cells into the media

RIES cell treatment[a]	15(*S*)-HETE	PGE_2
	pmol × 10^6 cells	*pmol × 10^6 cells*
NS398 [0 μM]	0.50 ± 0.05	0.99 ± 0.07
NS398 [0 μM] + vitamin C	0.39 ± 0.05	0.95 ± 0.09
NS398 [55 μM]	0.30 ± 0.04	0.53 ± 0.01
NS398 [55 μM] + vitamin C	0.25 ± 0.01	0.50 ± 0.01
NS398 [110 μM]	<0.15	<0.10
NS398 [110 μM] + vitamin C	<0.15	<0.10

[a] Vitamin C concentrations were 0.1 mM.

Targeted Lipidomics Analysis of RIES Cells in the Presence of NS-398—The RIES cells were treated with NS-398 (see the supplemental material) in the absence or presence of vitamin C. LC/APCI/MRM/MS analysis of the cell culture medium revealed that there was a dose-dependent decrease in the concentrations of 15(*S*)-HETE and PGE_2. At a concentration of 55 μM NS-398, 15(*S*)-HETE and PGE_2 concentrations were reduced by almost 50% to 0.30 ± 0.04 and 0.53 ± 0.01 pmol/10^6 cells, respectively in the absence of vitamin C (Table I) and to 0.25 ± 0.01 and 0.50 ± 0.01 pmol/10^6 cells, respectively, in the presence of vitamin C (Table I). At a concentration of 110 μM NS-398, PGE_2 and 15(*S*)-HETE concentrations were below the lower limit of detection in the absence (Fig. 4, *a* and *e*) or presence of vitamin C (Fig. 5, *a* and *e*).

Targeted Lipidomics Analysis of Intact RIES Cells in the Presence of Aspirin—At a concentration of 200 μM aspirin 15(*S*)-HETE and PGE_2 concentrations were below the lower limit of detection of the assay. However, aspirin induced the formation of 15(*R*)-HETE at a concentration of 0.69 ± 0.01 pmol/10^6 cells. Vitamin C did not have any effect on aspirin-mediated 15(*R*)-HETE formation (Fig. 6*a*) or on the inhibition of 15(*S*)-HETE and PGE_2 biosynthesis (Fig. 6, *a* and *e*).

Analysis of Heptanone-Etheno-dGuo from Intact RIES Cells—DNA was isolated from RIES cells after 24 h of incubation in media containing 0.1% FBS. The DNA was subjected to enzyme hydrolysis in the presence of $^{15}N_5$-labeled heptanone-etheno-dGuo internal standard. A portion of hydrolysate was removed for the quantitation of normal bases, by which the amount of DNA was determined. The endogenous DNA adducts

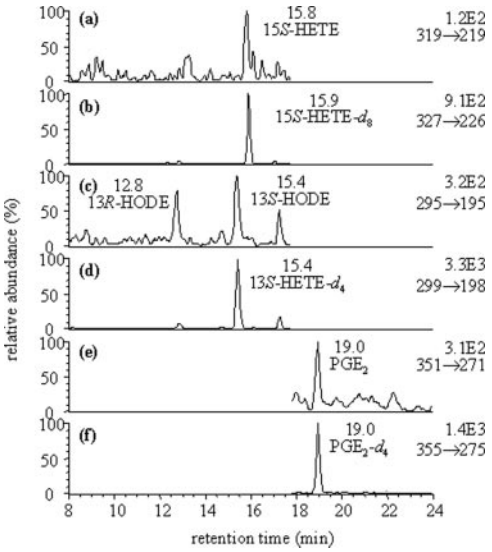

FIG. 3. **Targeted chiral lipidomics analysis of COX-2-derived AA and LA metabolites from RIES cells in the presence of vitamin C (0.1 mM).** MRM chromatograms are shown for 15(*R,S*)-HETE-PFB (*m/z* 319 → *m/z* 219) (*a*), 15(*S*)-[$^2H_8$]HETE-PFB internal standard (*m/z* 327 → *m/z* 226) (*b*), 13(*R,S*)-HODE-PFB (*m/z* 295 → *m/z* 195) (*c*), 13(*S*)-[$^2H_4$]HODE-PFB internal standard (*m/z* 299 → *m/z* 198) (*d*), PGE_2-PFB (*m/z* 351 → *m/z* 271) (*e*), [$^2H_4$]PGE_2-PFB internal standard (*m/z* 355 → *m/z* 275) (*f*).

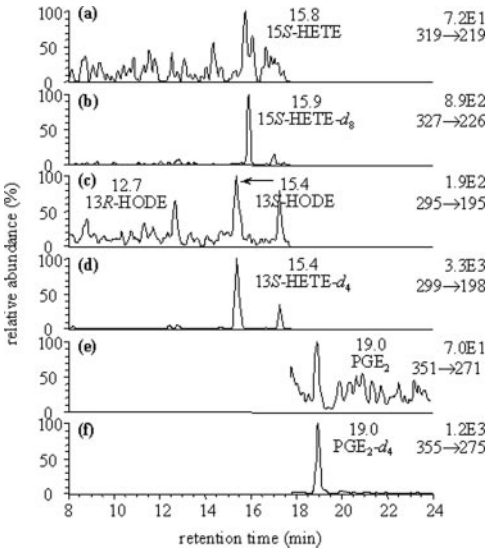

FIG. 4. **Targeted chiral lipidomics analysis of COX-2-derived AA and LA metabolites from RIES cells in the presence of NS-398 (110 μM).** The signals appearing in the endogenous channels arose from minor contamination of the deuterated standard by the protium form and from minor amounts of endogenous interfering substances present in the media. MRM chromatograms are shown for 15(*R,S*)-HETE-PFB (*m/z* 319 → *m/z* 219) (*a*), 15(*S*)-[$^2H_8$]HETE-PFB internal standard (*m/z* 327 → *m/z* 226) (*b*), 13(*R,S*)-HODE-PFB (*m/z* 295 → *m/z* 195) (*c*), 13(*S*)-[$^2H_4$]HODE-PFB internal standard (*m/z* 299 → *m/z* 198) (*d*), PGE_2-PFB (*m/z* 351 → *m/z* 271) (*e*), [$^2H_4$]PGE_2-PFB internal standard (*m/z* 355 → *m/z* 275) (*f*).

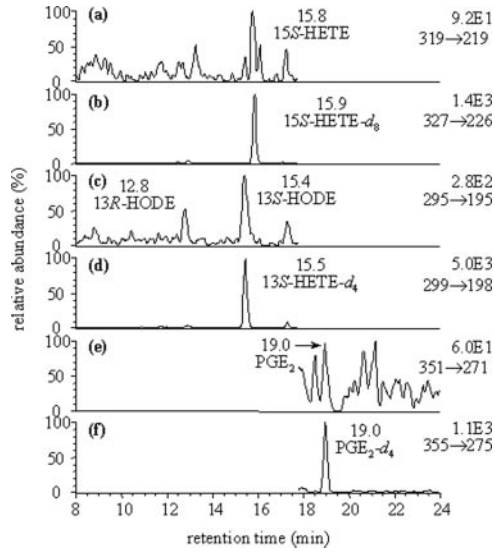

FIG. 5. **Targeted chiral lipidomics analysis of COX-2-derived AA and LA metabolites from RIES cells in the presence of vitamin C (0.1 mM) and NS-398 (110 μM).** The signals appearing in the endogenous channels arose from minor contamination of the deuterated standard by the protium form and from minor amounts of endogenous interfering substances present in the media. MRM chromatograms are shown for 15(*R,S*)-HETE-PFB (*m/z* 319 → *m/z* 219) (*a*), 15(*S*)-[$^2H_8$]HETE-PFB internal standard (*m/z* 327 → *m/z* 226) (*b*), 13(*R,S*)-HODE-PFB (*m/z* 295 → *m/z* 195) (*c*), 13(*S*)-[$^2H_4$]HODE-PFB internal standard (*m/z* 299 → *m/z* 198) (*d*), PGE_2-PFB (*m/z* 351 → *m/z* 271) (*e*), [$^2H_4$]PGE_2-PFB internal standard (*m/z* 355 → *m/z* 275) (*f*).

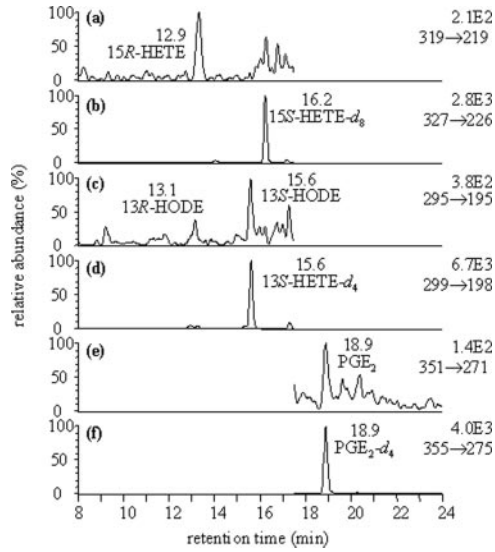

FIG. 6. **Targeted chiral lipidomics analysis of COX-2-derived AA and LA metabolites from RIES cells in the presence of vitamin C (0.1 mM) and aspirin (200 μM).** MRM chromatograms are shown for 15(*R,S*)-HETE-PFB (*m/z* 319 → *m/z* 219) (*a*), 15(*S*)-[$^2H_8$]HETE-PFB internal standard (*m/z* 327 → *m/z* 226) (*b*), 13(*R,S*)-HODE-PFB (*m/z* 295 → *m/z* 195) (*c*), 13(*S*)-[$^2H_4$]HODE-PFB internal standard (*m/z* 299 → *m/z* 198) (*d*), PGE_2-PFB (*m/z* 351 → *m/z* 271) (*e*), [$^2H_4$]PGE_2-PFB internal standard (*m/z* 355 → *m/z* 275) (*f*).

were isolated using solid phase extraction from the remaining hydrolysate. The heptanone-etheno-dGuo adduct and its $^{15}N_5$ internal standard were then converted to PFB derivatives to improve their positive APCI ionization characteristics (Fig. 7*A*). LC/MS/MS in the MRM mode was conducted on heptanone-etheno-dGuo-PFB (*m/z* 584 → *m/z* 468) and $^{15}N_5$-labeled heptanone-etheno-dGuo-PFB (*m/z* 589 → *m/z* 473). A typical regression line for heptanone-etheno-dGuo over the range of 0.05–5 pg/ml was $y = 0.5012\times - 0.0041$ ($r^2 = 0.9993$). The assay was validated by demonstrating for replicate quality control samples a precision of better than ±15% and accuracy between 85 and 115% on three separate days. The limit of detection was 0.05 pg/ml (precision was better than ±20%, and accuracy was between 80 and 120% on three separate days). When the authentic standard of heptanone-etheno-dGuo was analyzed with its $^{15}N_5$ internal standard, they eluted at the same retention time of 24.6 min (Fig. 7*A*). A typical chromatogram for the RIES cell-derived DNA adduct and its internal standard is shown in Fig. 7*B*. The DNA adducts were quantified using a calibration curve and normalized by the amount of DNA that was extracted from the RIES

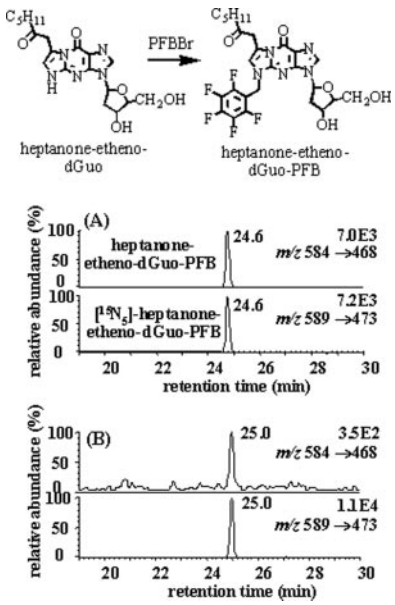

FIG. 7. *A*, LC/positive ion APCI/MRM chromatograms for authentic heptanone-etheno-dGuo-PFB (*m/z* 584 → *m/z* 468; *upper*) and $^{15}N_5$-labeled-heptanone-etheno-dGuo-PFB internal standard (*m/z* 589 → *m/z* 473; *lower*). *B*, LC/positive ion APCI/MRM chromatograms for heptanone-etheno-dGuo-PFB (*m/z* 584 → *m/z* 468; *upper*) isolated from RIES cell DNA incubated in the presence of vitamin C (0.1 mM) and $^{15}N_5$-labeled heptanone-etheno-dGuo-PFB internal standard (*m/z* 589 → *m/z* 473; *lower*).

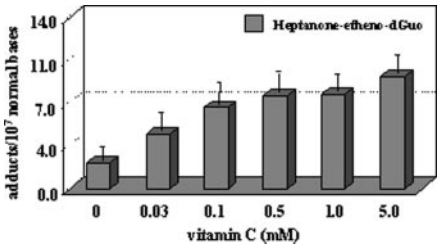

FIG. 8. **Amount of heptanone-etheno-dGuo (adducts/10^7 normal bases) in RIES cell DNA in the presence of increasing concentrations of vitamin C.** Determinations were conducted in triplicate (mean ± S.E.).

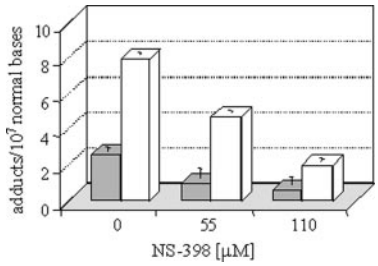

FIG. 9. **Amount of heptanone-etheno-dGuo (adducts/10^7 normal bases) in RIES cell DNA in the presence of increasing concentrations of NS-398.** Incubations were conducted in triplicate (mean ± S.E.) in the absence of vitamin C (*gray bars*) and the presence of 0.1 mM vitamin C (*open bars*).

cells. In the absence of vitamin C, heptanone-etheno-dGuo levels were 2.1 adducts/10^7 normal bases (Fig. 8).

Analysis of Heptanone-Etheno-dGuo from Intact RIES Cells Incubated with Vitamin C—RIES cells were treated with increasing amounts of vitamin C. As described above, after 24 h of incubation, the DNA was extracted and hydrolyzed. Endogenous DNA adducts were then isolated and converted to PFB derivatives for LC/APCI/MS analysis. A dose-dependent increase in DNA adduct formation was observed in the presence of vitamin C. At a concentration of 0.1 mM vitamin C, the level of heptanone-etheno-dGuo was increased over 3-fold to 6.6 adducts/10^7 normal bases from the basal level of 2.1 adducts/10^7 normal bases. Maximal adduct formation was observed with 1 mM vitamin C where the DNA adduct levels were 7.7 adducts/10^7 normal bases (Fig. 8).

Analysis of Heptanone-Etheno-dGuo from Intact RIES Cells Incubated with NS-398—RIES cells were treated with two different concentrations of the selective COX-2 inhibitor NS-398 in the absence or in the presence of vitamin C (0.1 mM). NS-398 caused a dose-dependent decrease in heptanone-etheno-dGuo adducts in the absence of vitamin C (Fig. 9). At concentrations of 55 and 110 μM NS-398, heptanone-etheno-dGuo levels were reduced to 1.0 and 0.7 adducts/10^7 normal bases, respectively. In the presence of vitamin C, the DNA adduct levels were 7.7, 4.8, and 1.8 adducts/10^7 normal bases for NS-398 concentrations of 0, 55, and 110 μM, respectively (Fig. 9).

Analysis of Heptanone-Etheno-dGuo from Intact RIES Cells Incubated with Aspirin—At a concentration of 200 μM aspirin, heptanone-etheno-dGuo levels were reduced to 0.5 adducts/10^7 normal bases. Vitamin C did not significantly affect the inhibition of adduct formation induced by 200 μM aspirin.

Artifact Formation during Isolation and Analysis of Heptanone-Etheno-dGuo—The artifactual formation of heptanone-etheno-dGuo was examined by adding $^{15}N_5$,$^{13}C_{10}$-labeled dGuo together with the internal standard $^{15}N_5$-labeled-heptanone-etheno-dGuo at the beginning of the DNA isolation procedure (see the supplemental material). The internal standard $^{15}N_5$-labeled-heptanone-etheno-dGuo was detected at the retention time of 25.0 min with MRM transition of *m/z* 589 → *m/z* 473. However, no $^{15}N_5$,$^{13}C_{10}$-labeled heptanone-etheno-dGuo was detected in the MRM channel of *m/z* 599 → *m/z* 478.

Targeted Lipidomics Analysis of RIES Cell Lysates with Increasing Concentrations of AA—The RIES cell lysates were treated with increasing concentrations of AA for 30 min at 37 °C, and the product profiles were analyzed by stable isotope dilution chiral LC/electron capture APCI/MS (see the supplemental material). 11(*R*)-HETE was the major product at all AA concentrations used (Fig. 10). The next most abundant metabolite was PGE_2 followed by 15(*S*)-HETE and 15(*R*)-HETE. At low AA concentrations there was only slightly more 11(*R*)-HETE than PGE_2. However, as the concentration of AA increased there was a gradual increase in the ratio of 11(*R*)-HETE to PGE_2. In contrast, the relative amounts of 11(*R*)-HETE and 15-HETEs were almost constant. The ratio of 15(*S*)-HETE (58%) to 15(*R*)-HETE (42%) was also constant from 1 to 100 μM AA.

Targeted Lipidomics Analysis of Calcium Ionophore-treated Intact RIES Cells—Cells were treated with calcium ionophore A23187 for 1 h at 37 °C, and the product profiles were analyzed by stable isotope dilution chiral LC/electron capture APCI/MS using the method described for the cell lysates. Quantitation of the lipids from three separate incubations of the RIES cells treated with calcium ionophore showed the presence of 11(*R*)-HETE (2.9 ± 0.16 pmol/10^6 cells), 15(*R*)-HETE (0.9 ± 0.05 pmol/10^6 cells), 15(*S*)-HETE (1.0 ± 0.07 pmol/10^6 cells), and PGE_2 (2.3 ± 0.11 pmol/10^6 cells). The relative amounts of 15(*S*)-HETE and 15(*R*)-HETE were 54 and 46%, respectively. Complete inhibition of HETE and PGE_2 production occurred on treatment with 110 μM NS-398.

Analysis of PGE_2 in WT RIE Cells—Standard curves were constructed for PGE_2 on three separate days in the range 0.67 pg/ml (0.002 pmol/ml) to 66.7 pg/ml (0.2 pmol/ml) (see the supplemental material). The assay was validated by showing for replicate quality control samples a precision of better than ±15% and accuracy between 85 and 115% on three separate days. The limit of detection for PGE_2 was 0.01 pmol/10^6 cells

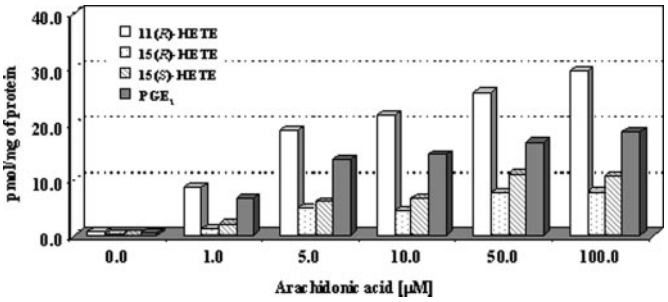

FIG. 10. **Amounts of 11-HETE, 15-HETE, and PGE_2 (pmol/mg of protein) formed after adding increasing concentrations of AA to RIES cell lysates.** Analyses were conducted in duplicate by stable isotope dilution LC/electron capture APCI/MRM/MS of PFB derivatives.

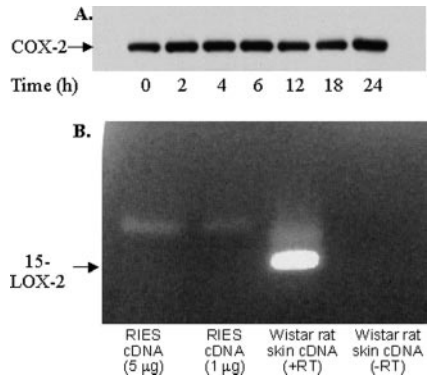

FIG. 11. *A*, Western blot analysis of COX-2 protein from RIES cells at different times after changing the media containing 10% FBS to media containing only 0.1% FBS. *B*, RT-PCR analysis of 15-LOX-2 in RIES cells. The expected 234-bp amplification product was found in Wistar rat skin cDNA used as the positive control. No amplification of 15-LOX-2 was observed from either the 1- or 5-μg samples obtained from RIES cell preparations.

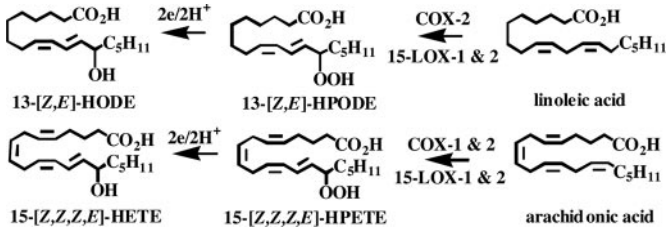

SCHEME 2. **COX-2-mediated formation of lipid hydroperoxides.**

(precision better than ±20%, and accuracy between 80 and 120% on three separate days). A typical regression line for PGE_2 was $y = 0.0045x + 0.0071$ ($r^2 = 0.9983$). Quantitation of PGE_2 from three separate incubations of the WT RIE cells showed the presence of 0.18 ± 0.002 pmol/10^6 cells. When WT RIE cells were treated with 110 μM NS-398 for 24 h at 37 °C, there was no significant difference in the concentrations of PGE_2 at 0.15 ± 0.003 pmol/10^6 cells ($n = 3$).

Western Blot Analysis of RIES Cells during 24 h of Incubation—During 24 h of incubation the amount of COX-2 protein remained constant (Fig. 11*A*).

RT-PCR Analysis of 15-LOX-2 in RIES Cells—The expected 234-bp amplification product was found in Wistar rat skin cDNA, used as the positive control (Fig. 11*B*). However, no amplification of 15-LOX-2 was observed from either the 1- or 5-μg samples obtained from RIES cell preparations (Fig. 11*B*).

DISCUSSION

A targeted chiral lipidomics analysis of the RIES cell media revealed that the major hydroxylated polyunsaturated fatty acid was 15(*S*)-HETE with a trace amount of 15(*R*)-HETE (Fig. 1). Retention times of the analytes relative to their deuterated internal standards were identical to those obtained from a standard mixture (Fig. 2). For example the relative retention times of 15(*R*)-HETE and 15(*S*)-HETE to the relevant 15(*S*)-[$^2H_4$]HETE internal standard were 0.79 ± 0.01 and 0.99 ± 0.01, respectively. As predicted for normal phase chromatography, 15(*S*)-HETE eluted with a slightly shorter retention time than the deuterated 15(*S*)-HETE analog.

These data suggested that the predominant lipid hydroperoxide formed by RIES cells was 15(*S*)-HPETE. No COX-2-derived 13(*S*)-HODE was detected, which indicated that 13(*S*)-HPODE did not contribute to DNA adduct formation (Scheme II). As expected, PGE_2 was also secreted by the RIES cells into the media (Fig. 1) together with small amounts of $PGF_{2\alpha}$ (data not shown). Quantitatively, there were approximately two times as much PGE_2 secreted as 15(*S*)-HETE (Table I). Incubation of the cells with 0.1 mM vitamin C resulted in a reduction of 15(*S*)-HETE, suggesting that some of the 15(*S*)-HPETE had been converted to bifunctional electrophiles (12) rather than to 15(*S*)-HETE (Scheme I). Treatment of the cells with the selective COX-2 inhibitor NS-398 in the absence of vitamin C resulted in a dose-dependent decrease in both 15(*S*)-HETE and PGE_2 formation (Table I). This implied that COX-2-mediated 15(*S*)-HPETE formation was also decreased. NS-398 at a concentration of 55 μM caused a reduction in both 15(*S*)-HETE and PGE_2 biosynthesis in the presence of 0.1 mM vitamin C (Table I). 15(*S*)-HETE and PGE_2 formation was completely inhibited at 110 μM NS-398 in the absence (Fig. 4) or presence of vitamin C (Fig. 5).

When the RIES cells were incubated with aspirin in the absence or presence of vitamin C, both PGE_2 and 15(*S*)-HETE biosynthesis were completely inhibited (Fig. 6). However, 15(*R*)-HETE was detected in amounts that were slightly higher than the original 15(*S*)-HETE that was observed in the absence of aspirin. This occurred in the absence or in the presence of vitamin C. Previous studies have required the use of exogenous AA either added to cells or to purified enzyme preparations to characterize this change in enantio-selectivity (Table II). Therefore, our new electron capture APCI methodology has confirmed that 15(*R*)-HETE and its presumed precursor 15(*R*)-HPETE are formed from endogenous AA in aspirin-treated cells that express the COX-2 enzyme.

DNA was isolated from RIES cells that had been incubated for 24 h in media containing 0.1% FBS and then hydrolyzed in the presence of $^{15}N_5$-labeled-heptanone-etheno-dGuo internal standard. The ONE-derived heptanone-etheno-dGuo adduct and its $^{15}N_5$-labeled internal standard were then converted to PFB derivatives to improve their positive APCI ionization characteristics. LC/APCI/MS/MS in the MRM mode was then conducted to provide maximal sensitivity and specificity. In separate experiments it was shown that heptanone-etheno-dGuo was not generated as an artifact during the DNA isolation, hydrolysis, and derivatization procedure. A typical chromatogram for the RIES cell-derived DNA adduct and its stable isotope internal standard is shown in Fig. 7*B*. In the absence of vitamin C, heptanone-etheno-dGuo levels were 2.1 adducts/10^7 normal bases (Fig. 8). A dose-dependent increase in DNA adduct formation was observed in the presence of vitamin C. Maximal adduct formation was observed with 1 mM vitamin C where there was a more than 3-fold increase in DNA adduct levels (Fig. 8). The selective COX-2 inhibitor NS-398 caused a dose-dependent decrease in heptanone-etheno-dGuo adducts in the absence of vitamin C (Fig. 9). However, in the presence of vitamin C, NS-398 was unable to reduce the formation of DNA adduct to base-line levels (Fig. 9).

Enantio-selectivity of COX-mediated 15-HETE formation

TABLE II
Chirality of 15-HETE formation from COX enzymes

Enzyme	Source	Species	Substrate	Additives	15-HETE chirality		Reference
					R	*S*	
COX-1	Partially purified	Ovine	[^{14}C]AA	Hematin, tryptophan, *p*-hydroxymercuribenzoate	77	33	6
COX-1	Partially purified	Ovine	[^{14}C]AA	Phenol, bovine hemoglobin	30	70	7
COX-1	Recombinant	Human	[^{14}C]AA	Hematin, phenol	33	67	8
COX-2	Recombinant	Human	AA	Heme, tryptophan	100	0	43
COX-2	Recombinant	Mouse	[^{14}C]AA	Hematin, phenol	28	72	8
COX-2	Recombinant	Human	[^{14}C]AA	Hematin, phenol	14	86	8
COX-2	Up-regulated	Ovine	[^{3}H]AA	Aspirin	75	25	44
COX-2	Transfected Cos-1 cells	Human	[^{14}C]AA	Aspirin	100	0	45
COX-2	Recombinant	Human	AA	Hematin, phenol, aspirin	100	0	46
COX-2	Recombinant	Human	AA	Heme, tryptophan, aspirin	100	0	43
COX-2	Purified	Mouse	[^{14}C]AA	Hematin, phenol, aspirin	>99	<1	47
COX-2	Recombinant	Mouse	[^{14}C]AA	Hematin, phenol, aspirin	>99	<1	48

has previously been determined in recombinant enzymes or in intact cells after the addition of AA (Table II). There is no consensus on the enantio-selectivity of either COX-1 or COX-2. Hecker *et al.* (6) showed that ovine COX-1 produced an excess of 15(*R*)-HETE, whereas Thuresson *et al.* (7) showed that it produced an excess of 15(*S*)-HETE (Table II). There is one report that human COX-2 forms enantiomerically pure 15(*R*)-HETE (43). This study also reported that aspirin did not affect the chirality of the 15-HETE that was formed. Another study showed that both mouse and human COX-2 formed more 15(*S*)-HETE than 15(*R*)-HETE (8). These findings suggest that the chirality of COX-mediated 15-HETE formation may be dependent upon the incubation conditions that are used. There is general agreement that both COX-1 and COX-2 produce enantiomerically pure 11(*R*)-HETE (7, 8, 43). Furthermore, it is generally agreed that 15(*R*)-HETE is the major HETE that is formed after aspirin treatment of COX-2 (43–48) (Table II). The initial step in 15(*R*)-HETE synthesis in acetylated COX-2 involves abstraction of the same pro-*S* hydrogen at C-13 of AA as occurs during normal PG biosynthesis (49). The change in oxygenation stereospecificity induced by aspirin treatment is proposed to arise because acetylated serine-516 in the human COX-2 (serine-530 in the mouse enzyme) forces a realignment of the ω-chain of AA. This unusual binding conformation appears to be responsible for oxygenation in the *R* configuration (43, 47–49).

No data exist on the relative amounts of HETE and PGE_2 formed by rat COX-2 or the chirality of rat COX-2-mediated HETE formation. To address these issues, HETEs and PGE_2 were quantified in RIES cell lysates treated with AA, and the chirality of the HETEs was determined. The presence of endogenous reducing co-factors in the lysates also helped to prevent the rapid inactivation of COX-2 that occurs in purified enzyme preparations 45–80 s after adding AA (50). 11(*R*)-HETE was the major metabolite at all AA concentrations used (Fig. 10). The next most abundant metabolite was PGE_2 followed by 15(*S*)-HETE and 15(*R*)-HETE. As the concentration of AA increased there was a gradual increase in the ratio of 11(*R*)-HETE to PGE_2. The ratio of 15(*S*)-HETE (58%) to 15(*R*)-HETE (42%) was constant from 1 to 100 μM AA. The preference for the 15(*S*) isomer was similar to that reported by Schneider *et al.* (8) for recombinant mouse and human COX-2, although the enantio-selectivity was somewhat lower (Table II).

There were some significant differences between the eicosanoids formed during incubations of intact RIES cells when compared with AA treatment of RIES cell lysates or with previous studies that examined AA treatment of recombinant COX-2 enzymes (Table II). The most surprising difference was the complete absence of 11(*R*)-HETE from the unstimulated incubations of intact RIES cells. This contrasts with our own work using cell lysates (Fig. 10) and with a number of studies using isolated enzymes showing that 11(*R*)-HETE is the major HETE generated by COXs (Table II). Interestingly, the enantio-selectivity observed for 15-HETE in the intact RIES cells was similar to that observed for recombinant mouse enzyme (Table II). In contrast, the ratio of PGE_2 to 15(*S*)-HETE (2:1) in intact RIES cells was similar to that observed at lower AA concentrations in the cell lysates. To further address this issue, eicosanoid production in the RIES cells from endogenous AA was induced using calcium ionophore A23187. This resulted in essentially the same pattern of metabolite formation, which occurred with AA treatment of the RIES cell lysates. It was particularly interesting that 11(*R*)-HETE was formed in concentrations that were similar to PGE_2. There is one previous study of COX-2-mediated biosynthesis of 11-HETE in intact cells (51). Eicosanoids were analyzed by achiral LC/MS after vigorous activation of COX-2 by a combination of both ionophore A23187 and AA in human lung adenocarcinoma A549 cells. Under these conditions 11-HETE and PGE_2 were released into the cell supernatant at concentrations of 24 and 127 pmol/10^6 cells, respectively (ratio 1:5). Therefore, substantially more PGE_2 was formed than from simple ionophore A23187 treatment of the RIES cells, but significant amounts of 11-HETE were also formed.

There was a striking difference in basal 15-HETE production in intact RIES cells when compared with AA treatment of isolated recombinant enzymes or cells in which COX-2 was highly up-regulated (Table II). The absence of 11(*R*)-HETE and the relatively small amount of 15(*R*)-HETE formed by the unstimulated intact RIES cell incubations suggests that they or their hydroperoxide precursors can undergo further metabolism. In fact there are several reports describing the metabolism of other HETE and HPETE regioisomers (52, 53).

A previous study with cultured ovine tracheal epithelial cells in which COX-2 had been up-regulated by growth factors quantified the relative amounts of 15-HETE and PGE_2 produced by adding [^{3}H]AA to washed cell suspensions (44). The ratio of 15-HETE to PGE_2 was 1:15. In a separate study [^{14}C]AA was added to Cos-1 cells transiently transfected with human COX-2 (54). No 15-HETE was detected, but 29.4% of the added [^{14}C]AA was converted to PGE_2. This extremely high rate of AA conversion contrasts with intact RIES cells and cell lysates, where the conversion of AA to PGE_2 was almost 3 orders of magnitude lower.

The significant differences in the ratio of 15-HETE and PGE_2 (1:2) in the RIES cells when compared with ovine epithelial cells (ratio 1:15) and Cos-1 cells transfected with human COX-2 (no 15-HETE detected) most likely arise because of the greatly

increased COX-2 activity in the latter two cell systems. Eicosanoid product profiles are highly dependent upon the length of time it takes for self-inactivation of the enzyme to occur. In isolated COX enzymes this takes place 45–80 s after AA addition, depending on the reducing co-factors that are present to protect the enzyme (50). For example, in studies with purified COX-1 from rat seminal vesicles (7), 15-HETE formation was maximal after 20 s, although PGE_2 concentrations increased for another 80 s. The ratio of 15-HETE to PGE_2 10 s after the addition of AA was 1:2, whereas after 100 s the ratio was 1:8 (7).

In microsomes from COS-7 cells transiently infected with recombinant COX-2, the ratio of 15-HETE to PGE_2 formation was 1:16 after a 30-min incubation (46). This is similar to the ratio observed in the ovine tracheal epithelial cells in which COX-2 had been up-regulated (44). It is noteworthy that the 15-HETE to PGE_2 ratio was increased by a factor of 2.5 in freshly isolated ovine tracheal epithelial cells where there was an almost 4-fold lower capacity for PGE_2 biosynthesis compared with the cells with up-regulated COX-2 (44). Furthermore, in human nasal polyp epithelial cells, which naturally express COX-2 rather than COX-1, the ratio of 15-HETE to PGE_2 was close to 1:1 (55). In intact unstimulated RIES cells and ionophore A23187-treated RIES cells, we determined that the ratio of 15-HETE to PGE_2 was 1:2 and 1:1, respectively. This is consistent with the ratio we found in RIES cell lysates and with the ratio of 15-HETE to PGE_2 that was found in human nasal polyp epithelial cells (55). Therefore, when cellular COX-2 levels are closer to those normally found under physiological conditions, it appears that both 15-HETE and PGE_2 are major metabolites.

The IC_{50} values of NS-398 for rat COX-2 and COX-1 have not been determined. IC_{50} values for recombinant ovine COX-2 and COX-1 are 0.15 and 220 μM, respectively (56). Therefore, the selectivity of COX-2 to COX-1 inhibition for NS-398 is >1000:1. To completely inhibit rat COX-2 in cell culture systems, NS-398 concentrations in the range 50–100 μM have generally been required (57–60). These concentrations are still well below the IC_{50} for recombinant ovine COX-1. Using a more sensitive LC/electron capture APCI/MS method, no NS-398 inhibition of PGE_2 formation was observed in WT RIE cells treated with 110 μM NS-398. This contrasts with complete inhibition observed in RIES cells, where more than five times as much PGE_2 was produced. Our findings are consistent with the rank order of potency described for the NS-398-mediated inhibition of eicosanoid biosynthesis by recombinant ovine COX-2 (56) and cellular rat COX-2 (57–60). These data taken together with the low PGE_2 biosynthesis by WT RIE cells, which only express COX-1, confirmed that the primary source of eicosanoids in the RIES cells was COX-2. In our earlier study with un-stimulated intact RIES cells (41), inhibition of 15(*S*)-HETE biosynthesis by NS-398 was not detected. However, no heavy isotope internal standard was used for 15-HETE. Seven heavy isotope internal standards were used in the present study including 15(*S*)-[$^2H_8$]HETE. Using this methodology it was unequivocally demonstrated that 15(*S*)-HETE is in fact a major COX-2 metabolite derived from RIES cells.

A Western blot analysis revealed that COX-2 expression was maintained for 24 h after the media containing 10% FBS had been replaced by media containing only 0.1% FBS (Fig. 11*A*). The possibility that RIES cells contained a 15-LOX activity that could be responsible for the formation of 15-HETE was considered. Human reticulocyte 15-LOX-1 and rat leukocyte-type 12/15-LOX are homologous genes in the two different species (61). Previous studies have demonstrated that 12-LOX is absent from the RIES cells. In fact the rat 12/15-LOX gene can be induced with sodium butyrate in WT RIE cells as demonstrated by the formation of 12- and 15-HETE (61). No 12-HETE was observed in butyrate-treated RIES cells. Similarly, 12-HETE was not formed in the present study of endogenous HETE formation by RIES cells. Therefore, RIES cells do not have any 12/15-LOX activity. In addition, RT-PCR was employed (Fig. 11*B*) to show that 15-LOX-2 mRNA was not present in the RIES cells (10). These data taken together with the inhibition of 15(*S*)-HETE biosynthesis by aspirin and NS-398 in the RIES cells established that it was derived from COX-2 and not 15-LOX-1 or 15-LOX-2.

Holtzman *et al.* (44) showed that aspirin could convert COX-2 to a 15(*R*)-LOX in ovine tracheal epithelial cells. The amount of 15-HETE was increased more than 4-fold in aspirin-treated cells when compared with untreated cells. However, 25% of the 15-HETE was accounted for by 15(*S*)-HETE. Therefore, the increase in 15(*R*)-HETE was actually 3.3-fold, which is similar to the 1.5-fold increase we observed in the aspirin-treated intact RIES cells. The identification of 15(*R*)-HETE suggested that significant amounts of 15(*R*)-HPETE had also been formed. 15(*R*)-HPETE should give rise to exactly the same amount of heptanone-etheno-dGuo as its 15(*S*)-enantiomer (12). Therefore, it was somewhat surprising that no increase in heptanone-etheno adduct formation occurred in the aspirin-treated RIES cells. In contrast, the expected aspirin-mediated inhibition of PGE_2 biosynthesis was observed both in the absence and presence of vitamin C (Fig. 6). This occurs through acetylation of serine 516 in the human enzyme (49), which inhibits formation of the hydroperoxide products PGG_2 and 11(*R*)-HPETE. Aspirin-mediated inhibition of these pathways could spare cellular reducing equivalents that would then be available to convert the resulting 15(*R*)-HPETE into 15(*R*)-HETE and so prevent the formation of heptanone-etheno adducts. In keeping with this possibility, we have shown recently that low μM concentrations of lipid hydroperoxide-derived bifunctional electrophiles can rapidly reduce intracellular glutathione levels with concomitant formation of glutathione adducts (63). Therefore, aspirin appears to have an additional activity within the cell through acting in effect as an antioxidant that prevents COX-2-mediated formation of a lipid hydroperoxide (15(*R*)-HPETE), which can undergo homolytic decomposition to genotoxic bifunctional electrophiles.

Concentrations of vitamin C used in the present study are comparable to those found in human subjects (64). The efficiency with which vitamin C could induce lipid hydroperoxide decomposition to bifunctional electrophiles *in vitro* suggested that this process could induce significant levels of DNA damage *in vivo* (11). We have now demonstrated that this process can indeed occur when COX-2 is permanently expressed in RIES cells. The finding that vitamin C causes an increase in lipid hydroperoxide-mediated DNA adduct formation could help to explain why vitamin C has not been effective in cancer chemoprevention trials when used as a single agent (65). COX-2 is up-regulated in many tumor tissues (38), and a number of studies have been conducted to determine precisely how COX-2 mediates tumorigenesis. Current research suggests that it is involved cellular proliferation, angiogenesis, resistance to apoptosis, enhancing invasiveness, and modulation of immunosuppression (66). These biological activities are thought to result primarily through the formation of PGs such as PGE_2. The present study provides evidence for an additional mechanism that may be involved in tumorigenesis; namely, the formation of etheno-DNA adducts that arise as a consequence of COX-2-mediated lipid peroxidation (Scheme I). Under most circumstances lipid hydroperoxide-derived etheno-DNA adducts are repaired from the DNA. When there is a reduced capacity for

DNA repair or when repair processes are overwhelmed, the etheno-DNA adducts could be responsible for increased mutagenesis and carcinogenesis (62). Therefore, inhibition of COX-2-mediated lipid hydroperoxide formation offers a potential therapeutic alternative to conventional COX-2 inhibitors in chemoprevention strategies for human populations.

Acknowledgment—We thank Thermo Electron for the loan of a Finnigan TSQ Ultra AM tandem mass spectrometer.

REFERENCES

1. Laneuville, O., Breuer, D. K., Xu, N., Huang, Z. H., Gage, D. A., Watson, J. T., Lagarde, M., DeWitt, D. L., and Smith, W. L. (1995) *J. Biol. Chem.* **270,** 19330–19336
2. Hamberg, M. (1998) *Arch. Biochem. Biophys.* **349,** 376–380
3. Brash, A. R. (1999) *J. Biol. Chem.* **274,** 23679–23682
4. Porter, N. A., Caldwell, S. E., and Mills, K. A. (1995) *Lipids* **30,** 277–290
5. Kuhn, H., and Borchert, A. (2002) *Free Radic. Biol. Med.* **33,** 154–172
6. Hecker. M., Ullrich, V., Fischer, C., and Meese, C. O. (1987) *Eur. J. Biochem.* **169,** 113–123
7. Thuresson, E. D., Lakkides, K. M., and Smith, W. L. (2000) *J. Biol. Chem.* **275,** 8501–8507
8. Schneider, C., Boeglin, W. E., Prusakiewicz, J. J., Rowlinson, S. W., Marnett, L. J., Samel, N., and Brash, A. R. (2002) *J. Biol. Chem.* **277,** 478–485
9. Ikawa, H., Kamitani, H., Calvo, B. F., Foley, J. F., and Eling, T. E. (1999) *Cancer Res.* **59,** 360–366
10. Brash, A. R., Boeglin, W. E., and Chang, M. S. (1997) *Proc. Natl. Acad. Sci. U. S. A.* **94,** 6148–6152
11. Lee, S. H., Oe, T., and Blair, I. A. (2001) *Science* **292,** 2083–2086
12. Williams, M. V., Lee, S. H., and Blair, I. A. (2005) *Rapid Commun. Mass Spectrom.* **19,** 849–858
13. Jian, W., Lee, S. H., Arora, J. S., Silva Elipe, M. V., and Blair, I. A. (2005) *Chem. Res. Toxicol.* **18,** 599–610
14. Lee, S. H., Elipe, M. V. S., Arora, J. S., and Blair, I. A. (2005) *Chem. Res. Toxicol.* **18,** 566–578
15. Kawai, Y., Uchida, K., and Osawa, T. (2004) *Free Radic. Biol. Med.* **36,** 529–541
16. Pryor, W. A., and Stanley, J. P. (1975) *J. Org. Chem.* **40,** 3615–3617
17. Lee, S. H., Oe, T., and Blair, I. A. (2002) *Chem. Res. Toxicol.* **15,** 300–304
18. Schneider, C., Tallman, K. A., Porter, N. A., and Brash, A. R. (2001) *J. Biol. Chem.* **276,** 20831–20838
19. Lee, S. H., and Blair, I. A. (2000) *Chem. Res. Toxicol.* **13,** 698–702
20. Gallasch, B. A. W., and Spiteller, G. (2000) *Lipids* **35,** 953–960
21. Rindgen, D., Nakajima, M., Wehrli, S., Xu, K., and Blair, I. A. (1999) *Chem. Res. Toxicol.* **12,** 1195–1204
22. Rindgen, D., Lee, S. H., Nakajima, M., and Blair, I. A. (2000) *Chem. Res. Toxicol.* **13,** 846–852
23. Lee, S. H., Rindgen, D., Bible, R. A., Hajdu, E., and Blair, I. A. (2000) *Chem. Res. Toxicol.* **13,** 565–574
24. Pollack, M., Oe, T., Lee, S. H., Silva Elipe M. V., Arison, B. H., and Blair, I. A. (2003) *Chem. Res. Toxicol.* **16,** 893–900
25. Lee, S. H., Oe, T., Arora, J. S., and Blair, I. A. (2005) *Chem. Res. Toxicol.* **18,** 780–786
26. Akasaka, S., and Guengerich, F. P. (1999) *Chem. Res. Toxicol.* **12,** 501–507
27. Levine, R. L., Yang, I.-Y., Hossain, M., Pandya, G., Grollman, A. P., and Moriya, M. (2000) *Cancer Res.* **60,** 4098–4104
28. Douki, T., Odin, F., Caillat, S., Favier, A., and Cadet, J. (2004) *Free Radic. Biol. Med.* **37,** 62–70
29. Uchida, K. (2003) *Prog. Lipid Res.* **42,** 319–343
30. Oe, T, Lee, S. H., Silva Elipe, M. V., Arison, B. H., and Blair, I. A. (2003) *Chem. Res. Toxicol.* **16,** 1598–1605
31. Oe, T., Arora, J. S., Lee, S. H., and Blair, I. A. (2003) *J. Biol. Chem.*, **278,** 42098–43105
32. Liu, Z., Minkler, P. E., and Sayre, L. M. (2003) *Chem. Res. Toxicol.* **16,** 901–911
33. Zhang, W. H., Liu, J., Xu, G., Yuan, Q., and Sayre, L. M. (2003) *Chem. Res. Toxicol.* **16,** 512–552
34. Thun, M. J., Namboodiri, M. M., Calle, E. E., Flanders, W. D., and Heath, C. W., Jr. (1993) *Cancer Res.* **53,** 1322–1327
35. Thun, M. J., Henley, S. J., and Patrono, C. (2002) *J. Natl. Cancer Inst.* **94,** 252–266
36. Davies, G. L. (2003) *J. Steroid Biochem. Mol. Biol.* **86,** 495–499
37. Williams, C., Shattuck-Brandt, R. L., and DuBois, R. N. (1999) *Ann. N. Y. Acad. Sci.* **889,** 72–83
38. Gupta, R. A., and Dubois, R. N. (2001) *Nat. Rev. Cancer* **1,** 11–21
39. Tsujii M., and DuBois. R. N. (1995) *Cell* **83,** 493–501
40. DuBois, R. N., Shao, J., Tsujii, M., Sheng, H., and Beauchamp, R. D. (1996) *Cancer Res.* **56,** 733–737
41. Lee, S. H., Williams, M. V., DuBois, R. N., and Blair, I. A. (2003) *Rapid Commun. Mass Spectrom.* **17,** 2168–2176
42. Singh, G., Gutierrez, A., Xu, K., and Blair, I. A. (2000) *Anal. Chem.* **72,** 3007–3013
43. Xiao, G., Tsai, A. L., Palmer, G., Boyar, W. C., Marshall, P. J., and Kulmacz, R. J. (1997) *Biochemistry* **36,** 1836–1845
44. Holtzman, M. J., Turk, J., and Shornick, L. P. (1992) *J. Biol. Chem.* **267,** 21438–21445
45. Lecomte, M., Laneuville, O., Ji, C., DeWitt, D. L., and Smith, W. L. (1994) *J. Biol. Chem.* **269,** 13207–13215
46. O'Neill, G. P., Mancini, J. A., Kargman S., Yergey J., Kwan M. Y., Falgueyret, J. P., Abramovitz, M., Kennedy B. P., Ouellet M., Cromlish, W., Culp, S., Evans, J. F., Ford-Hutchinson, A. W., and Vickers, P. J. (1994) *Mol. Pharmacol.* **45,** 245–254
47. Rowlinson, S. W., Crews, B. C., Goodwin, D. C., Schneider, C., Gierse, J. K., and Marnett, L. J. (2000) *J. Biol. Chem.* **275,** 6586–6591
48. Schneider, C., and Brash, A. R. (2000) *J. Biol. Chem.* **275,** 4743–4746
49. Smith, W. L., Garavito, R. M., and DeWitt, D. L. (1996) *J. Biol. Chem.* **271,** 33157–33160
50. Szewczuk, L. M., Forti, L., Stivala, L. A., and Penning, T. M. (2004) *J. Biol. Chem.* **279,** 22727–22737
51. Kempen, E. C., Yang, P., Felix, E., Madden, T., and Newman, R. A. (2001) *Anal. Biochem.* **297,** 183–190
52. Zarini, S., and Murphy, R. C. (2003) *J. Biol. Chem.* **278,** 11190–11196
53. Yu, Z., Schneider, C., Boeglin, W. E., Marnett, L. J., and Brash, A. R. (2003) *Proc. Natl. Acad. Sci. U. S. A.* **100,** 9162–9167
54. Meade, E. A., Smith, W. L., and DeWitt, D. L. (1993) *J. Biol. Chem.* **268,** 6610–6614
55. Kowalski, M. L., Pawliczak, R., Wozniak, J., Siuda, K., Poniatowska, M., Iwaszkiewicz, J., Kornatowski, T., and Kaliner, M. A. (2000) *Am. J. Respir. Crit. Care Med.* **161,** 391–398
56. Johnson, J.L., Wimsatt, J., Buckel, S. D., Dyer, R. D., and Maddipati K. R. (1995) *Arch. Biochem. Biophys.* **324,** 26–34
57. Tran, P. O., Gleason, C. E., Poitout, V., and Robertson, R. P. (1999) *J. Biol. Chem.* **274,** 31245–31248
58. Boyle, J. E., Lindroos, P. M., Rice, A. B., Zhang L., Zeldin, D. C., and Bonner J. C. (1999) *Am. J. Respir. Cell Mol. Biol.* **20,** 433–440
59. Teather, L. A., and Wurtman, R. J. (2003) *Neurosci. Lett.* **340,** 177–180
60. Fernandez-Tome, M., Kraemer, L., Federman, S. C., Favale, N., Speziale, E., and Sterin-Speziale, N. (2004) *Biochem. Pharmacol.* **67,** 245–254
61. Kamitani, H., Ikawa H., Hsi L. C., Watanabe T, DuBois R. N., and Eling T. E. (1999) *Arch. Biochem. Biophys.* **368,** 45–55
62. Gros, L., Ishchenko, A. A., and Saparbaev, M. (2003) *Mutat. Res.* **531,** 219–229
63. Jian, W., Arora, J. S., Oe, T., Shuvaev, V. V., and Blair, I. A. (2005) *Free Rad. Biol. Med.*, in press
64. Levine, M., Conry-Cantilena, C., Wang, Y., Welch, R. W., Washko, P. W., Dhariwal, K. R., Park, J. B., Lazarev, A., Graumlich, J. F., King, J., and Cantilena, L. R. (1996) *Proc. Natl. Acad. Sci. U. S. A.* **93,** 3704–3704-3709
65. Lippman, S. M., Lee, J. J., and Sabichi, A. L. (1998) *J. Natl. Cancer Inst.* **90,** 1514–1528
66. Wang, D., and Dubois, R. N. (2004) *Semin. Oncol.* **31,** 64–73